Review

Development Perspective of bioelectrocatalysis-based biosensors

Taiki Adachi, Yuki Kitazumi, Osamu Shirai, Kenji Kano*,a)

1 Division of Applied Life Sciences, Graduate School of Agriculture, Kyoto University, Sakyo, Kyoto 606-8502, Japan.

* Correspondence: kano.kenji.5z@kyoto-u.ac.jp (K.K.)

a) Present address: Center for Advanced Science and Innovation, Kyoto University, Gokasho, Uji, Kyoto 611-0011, Japan

Abstract: Bioelectrocatalysis provides the intrinsic catalytic-functions of redox enzymes to non-specific electrode reactions and is the most important and basic concept for biosensors. This review starts by describing fundamental characteristics of bioelectrocatalytic reactions in mediated and direct electron transfer types from a theoretical viewpoint and summarizes amperometric biosensors based on multi-enzymatic cascades and for multi-analyte detection. The review also introduces prospective aspects of two new concepts of biosensors: mass-transfer-controlled (pseudo)steady-state amperometry at microelectrodes with enhanced enzymatic activity without calibration curves and potentiometric coulometry at enzyme/mediator-immobilized biosensors for absolute determination.

Keywords: current-potential curve; multi-enzymatic cascades; multi-analyte detection; mass-transfer-controlled amperometric response; potentiometric coulometry

1. Introduction

Electron transfer reactions such as photosynthesis, respiration, and metabolisms play an important role in all living things. A huge variety of redox enzymes catalyze the oxidation and reduction of couples of two inherent substrates. The electrons are transferred usually between the two substrates through a cofactor(s). The most important ones are pyridine nucleotide coenzymes (NAD(P)(H)). The coenzymes shuttle back and forth between NAD(P)-dependent enzymes and solution, and mediate hydride ion transfers (single step two-electron one-proton redox reactions) between two organic substrates in the biological system without generating any intermediate radicals. Flavin cofactors (FAD(H$_2$) FMN(H$_2$)) and quinone cofactors including pyrroloquinoline quinone (PQQ) can undergo both hydride ion and electron transfers. Molybdopterin cofactors (Mocos) have similar properties. These cofactors are covalently or non-covalently bound to redox enzymes. On the other hand, there are a variety of metallic ion cofactors, such as hemes, iron-sulfur clusters, copper ion, nickel ion, and manganese ion in redox enzymes. These metallic ion cofactors undergo electron transfers. Therefore, flavin and quinone cofactors and Mocos have very important roles to couple the hydride ion transfer system and the electron transfer system.

The coupling of redox enzymatic reactions with electrochemical reactions has received worldwide medical and scientific interests [1-14]. The coupled reaction is called bioelectrocatalysis. Since enzymatic reactions show very high performance in the selectivity, catalytic activity, uniformity, and enormous chemical versatility, the coupling provides those redox-enzymatic characteristics to non-specific electrode reactions. Therefore, several bioelectrochemical devices have been developed based on bioelectrocatalysis, such as biosensors [9,15], biological fuel cells [16-20], bioelectrochemical reactors [21,22], and biosupercapacitors [23].

Most of redox-enzymatic reactions can be coupled with electrode reactions by way of redox mediators [3,24-26]. This reaction is called mediated electron transfer (MET)-type bioelectrocatalysis.

Since electrode reactions are not hydride ion transfer, but electron transfer, NAD(P)-dependent enzymatic reactions have to be coupled to electrode reactions by using redox mediators that can transfer both hydride ion and electron, such as flavins, quinones (especially *o*-quinones), and phenothiazines (such as Meldola's blue). For other redox enzymes (that is, flavoenzymes, quinoenzymes, metal-containing enzymes), a large variety of redox compounds (that undergo electron transfers) including metallic complexes (such ferrocenes, ferrocyanide, osmium complexes) can be used as mediators.

On the other hand, it is known that some metal-containing enzymes and flavoenzymes can directly exchange electrons with electrodes in the absence of any mediators in the catalytic reaction. Such a reaction is referred to as direct electron transfer (DET)-type bioelectrocatalysis [14,27-31]. DET-type bioelectrocatalysis can simplify the fabrication of bioelectrodes, and can minimize the thermodynamic overpotential in the coupling reaction in theory. However, the number of redox enzymes that provide clear DET-type bioelectrocatalytic waves is limited, and DET-type reactions are very susceptible to the condition and structure of the electrode surface.

Amperometric biosensors on the basis of bioelectrocatalysis are analytical devices to detect specific target analytes (substrates) and have been widely used in various fields such as medical care, environmental monitoring, food safety, and industrial bioprocess monitoring [12,13,32,33]. Generally, there are many compounds (analytes) in the target fluid. Therefore, multi-analyte biosensors that may realize cost-effective and rapid analysis with reducing the volume of the sample have been improved [34]. When a single enzyme reaction cannot be effectively coupled with electrode reactions, multiple enzymes that work in a cascade mode are required. In this case, immobilization and co-localization of multiple enzymes are necessary for sensor electrodes, and various methods for immobilization and co-localization of multi-enzyme have been reported [35-37].

The response of an amperometric sensor, however, depends on the detection time, and it limits the practical application [4,9,11-13,26,32,33]. It is necessary for amperometric sensors to obtain steady-state currents. If one can use biosensors without calibration, it will become easy to monitor the concentration of target analytes. In this sense, microelectrode detection was introduced to develop amperometric biosensors [38-44]. Nonlinear diffusion of the substrate at microelectrodes causes diffusion-controlled steady-state currents. In addition, microelectrode-type biosensors are suitable for miniaturization and reducing the volume of samples. On the other hand, coulometry that can determine the absolute quantity is one of absolute analytical methods. However, non-Faradaic background electricity (background current integrated during absolute electrolysis) becomes too large to ignore compared with Faradaic electricity to be measured at decreased concentrations of analytes. In order to overcome this issue, potentiometric coulometry bases on MET-type bioelectrocatalysis has been proposed, in which the total electricity of an analyte in a small value of test solution was transferred to the mediator immobilized on an electrode and the change in the redox state of the mediator is potentiometrically detected [45,46].
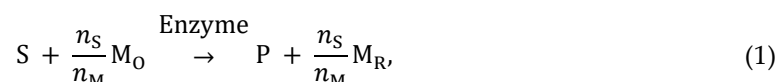
In this review, we will describe fundamental concepts of MET- and DET-type bioelectrocatalytic reactions, practical use of biosensors such as multi-enzyme biosensor and multi-analyte biosensor, and prospective biosensors which can be utilized without calibration.

2. Fundamentals of bioelectrocatalytic sensors

2.1. Theory of steady-state MET-type bioelectrocatalysis

2.1.1. MET-type bioelectrocatalysis in homogeneous system

In the MET-type bioelectrocatalysis (for the oxidation of a substrate (S) to a product (P)), the enzymatic reaction catalyzed by an enzyme (E) and the electrode reaction of a mediator (M) are coupled as follows:

$$S + \frac{n_S}{n_M} M_O \xrightarrow{\text{Enzyme}} P + \frac{n_S}{n_M} M_R, \tag{1}$$

and

$$\begin{array}{c} \text{Electrode} \\ M_R \quad \rightarrow \quad M_O + n_M e^-, \end{array} \qquad (2)$$

where n_X is the number of electrons of X. In the presence of the enzyme, the mediator, and the substrate in a quiescent solution, a 1D reaction-diffusion equation of the MET-type bioelectrocatalytic reaction under the steady-state conditions is expressed as follows:

$$\frac{\partial c_{M_O}}{\partial t} = D_M \frac{\partial^2 c_{M_O}}{\partial x^2} - \frac{n_S}{n_M} \frac{k_c c_E}{1 + \dfrac{K_M}{c_{M_O}} + \dfrac{K_S}{c_S}} = 0, \qquad (3)$$

where c_X is the concentration of X, t is the time, x is the distance from the electrode surface, D_M is the diffusion coefficient of the mediator, k_c is the catalytic constant, and K_X is the Michaelis constant for X, respectively. When the overpotential is high enough and the excess amount of S is present in solution ($c_S \gg K_S$), the limiting steady-state current ($i_{s,lim}$) can be obtained and is expressed by solving Eq. (3) [47]:

$$i_{s,lim} = FA \sqrt{2 n_S n_M D_M k_c K_M c_E \left\{ \frac{c_M}{K_M} - \ln\left(1 + \frac{c_M}{K_M}\right) \right\}}, \qquad (4)$$

where F is the Faraday constant, A is the electrode surface area, and $c_M \equiv c_{M_O} + c_{M_R}$, respectively. Furthermore, Eq. (4) is simplified in two limited cases of c_M; when $c_M \ll K_M$:

$$i_{s,lim} = FAc_M \sqrt{n_S n_M D_M \frac{k_c}{K_M} c_E}, \qquad (5)$$

and when $c_M \gg K_M$:

$$i_{s,lim} = FA\sqrt{2 n_S n_M D_M k_c c_E c_M}. \qquad (6)$$

2.1.2. Reaction-layer model at enzyme/mediator-immobilized electrodes

Enzymes and mediators are often immobilized on the electrode surface for the application to biosensors. In such situations, an enzyme/mediator-co-immobilized layer and a reaction layer must be considered.

When the enzyme/mediator-co-immobilized layer is sufficiently smaller in thickness than the reaction layer ($L \ll \mu$, L and μ being the thickness of immobilized and reaction layers, respectively), reaction (1) becomes the rate-determining step of the total reaction, and the concentration polarization of the mediator and the substrate becomes negligible. Introducing a reaction layer theory [48] under the conditions of large overpotentials and $c_S \gg K_S$, $i_{s,lim}$ is expressed as follows:

$$i_{s,lim} = FAn_S D_M \frac{k_c c_E}{1 + \dfrac{K_M}{c_{M_O}}} L. \qquad (7)$$

When $L \gg \mu$ or $L \approx \mu$, $i_{s,lim}$ is expressed as follows:

$$i_{s,lim} = FA\sqrt{2 n_S n_M D_M k_c c_E B} \tanh\left\{ \frac{L}{1 + \dfrac{K_M}{c_M}} \sqrt{\frac{n_S}{n_M} \frac{k_c c_E}{2 D_M K_M B}} \right\}, \qquad (8)$$

where $B = \frac{c_M}{K_M} - \ln\left(1 + \frac{c_M}{K_M}\right)$. Equation (8) is simplified in two limited cases of c_M, and μ is expressed as follows. When $c_M \ll K_M$,

$$i_{s,\text{lim}} = FAc_M \sqrt{n_S n_M D_M \frac{k_c}{K_M} c_E} \tanh\left(\frac{L}{\mu}\right), \tag{9}$$

$$\mu = \sqrt{\frac{n_S}{n_M} \frac{k_c c_E}{D_M K_M}}; \tag{10}$$

and when $c_M \gg K_M$,

$$i_{s,\text{lim}} = FA\sqrt{2n_S n_M D_M k_c c_E c_M} \tanh\left(\frac{L}{\mu}\right), \tag{11}$$

$$\mu = \sqrt{\frac{n_S}{n_M} \frac{k_c c_E}{2D_M c_M}}. \tag{12}$$

It is essential to optimize the value of *L*, in order to construct biosensors with large values of $i_{s,\text{lim}}/A$ using minimum amounts of enzymes and mediators.

2.1.3. Serial resistance model

The steady-state MET-type bioelectrocatalysis can be explained based on a serial resistance model. In this model, we assume a set of series reactions (Fig. 1): 1) mass transfer, 2) membrane permeation, 3) enzymatic reaction, and 4) electrode reaction. The steady-state current (i_s) can be expressed as follows:

$$\frac{1}{i_s} \cong \frac{1}{i_{mt}} + \frac{1}{i_{perm}} + \frac{1}{i_{enz}} + \frac{1}{i_{elec}}, \tag{13}$$

where i_{mt}, i_{perm}, i_{enz} and i_{elec} are the limiting steady-state currents controlled by mass-transfer, permeation, enzymatic reaction, and electrode reaction, respectively. i_{mt} is given by Levich equation at a rotating disk electrode (RDE) or by Eq. (15) at a microdisk electrode:

$$i_{mt,\text{RDE}} = \pm 0.620 n_S FAD_S^{\frac{2}{3}} \nu^{-\frac{1}{6}} \omega^{\frac{1}{2}} c_S, \tag{14}$$

$$i_{mt,\text{microdisk}} = \pm 4 n_S FD_S r c_S, \tag{15}$$

where D_S is the diffusion coefficient of the substrate, ν is a kinetic viscosity of the buffer solution, ω is an angular rotation rate of the RDE, and *r* is a radius of the microdisk electrode. i_{perm} can be expressed as follows:

$$i_{perm} = \pm n_S FAP_m c_S, \tag{16}$$

where P_m is a permeation coefficient of a membrane. i_{enz} is given by a Michaelis–Menten-type equation in the presence of an excess amount of a mediator as follows:

$$i_{enz} = \pm n_S FA \frac{k_c \Gamma_E}{1 + \frac{K_S}{c_S}}, \tag{17}$$

where Γ_E is the surface concentration of an enzyme. i_{elec} is given by a Butler–Volmer-type equation as follows:

$$i_{elec} = n_S FAk_M^\circ c_S \exp\left\{\frac{n_{M,\text{rds}} F}{RT} (E - E_{M,\text{rds}}^{\circ\prime})\right\}^{1-\alpha_{M,\text{rds}}}, \tag{18}$$

where k_M° is the standard rate constant in the rate-determining step (rds) of the interfacial electron transfer of the mediator at the electrode, *R* is the gas constant, *T* is the absolute temperature, $n_{M,\text{rds}}$ is the number of electrons in the rds of the mediator (generally $n_{M,\text{rds}} = 1$), *E* is the electrode potential,

$E_{\text{M,rds}}^{\text{o}\prime}$ is the formal potential of the rds of the mediator, and $\alpha_{\text{M,rds}}$ is the transfer coefficient in the rds of the mediator.

Under the condition of $E \gg E_{\text{M,rds}}^{\text{o}\prime}$, i_{elec} becomes sufficiently larger than i_{mt}, i_{perm}, and i_{enz} to give a steady-state limiting current. On the other hand, i_{perm} depends on an outer membrane and i_{enz} is directly affected by $k_{\text{c}}\Gamma_{\text{E}}$, which often varies under measurement conditions such as temperature and pH. Thus, a diffusion-controlled steady-state condition ($i_{\text{mt}} \ll i_{\text{perm}}$, i_{enz}, and i_{elec}) is ideal for amperometric biosensors, in which no calibration curve is required for determination.
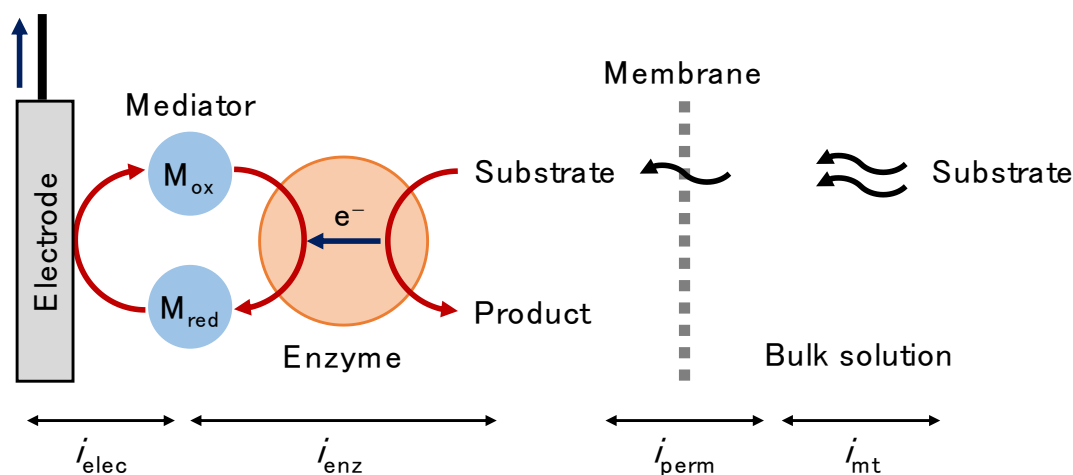

Figure 1.   A schematic view of MET-type bioelectrocatalysis based on a serial resistance model.

2.2. Theory of steady-state DET-type bioelectrocatalysis

In the DET-type bioelectrocatalysis, an enzyme reacts with both a substrate and an electrode as follows:

$$\text{S} + \text{E}_{\text{O}} \quad \overset{\text{Enzyme}}{\longrightarrow} \quad \text{P} + \text{E}_{\text{R}}, \tag{19}$$

$$\text{E}_{\text{R}} \quad \overset{\text{Electrode}}{\rightleftarrows} \quad \text{E}_{\text{O}} + n_{\text{E}}\text{e}^{-}, \tag{20}$$

In this situation, i_{s} can be expressed by the following equation based on the serial resistance model with a series of the mass-transfer process and the DET-type bioelectrocatalysis on the electrode surface (electro-enzyme reaction):

$$\frac{1}{i_{\text{s}}} = \frac{1}{i_{\text{mt}}} + \frac{1}{i_{\text{elec}-\text{enz}}}, \tag{21}$$

where i_{mt} is given by Eqs. (14) and (15) for RDE and microdisk electrode experiments, respectively. $i_{\text{elec-enz}}$ (the electro-enzyme reaction-controlled current) can be expressed as follows [49]:

$$i_{\text{elec}-\text{enz}} = \pm \frac{n_{\text{S}}FAk_{\text{c,DET}}\Gamma_{\text{E}}}{1 + \frac{k_{\text{c,DET}}}{k_{\text{f}}} + \frac{k_{\text{b}}}{k_{\text{f}}}}, \tag{22}$$

where $k_{\text{c,DET}}$ is the catalytic constant in DET-type bioelectrocatalysis, k_{f} and k_{b} are the interfacial electron transfer rate constants of forward and backward reactions, respectively, which are given by the Butler–Volmer equations as follows. For oxidation,

$$k_{\text{f}} = k_{\text{E}}^{\text{o}}\eta_{\text{E}}^{1-\alpha_{\text{E,rds}}} \tag{23}$$

$$k_{\text{b}} = k_{\text{E}}^{\text{o}}\eta_{\text{E}}^{-\alpha_{\text{E,rds}}}, \tag{24}$$

and for reduction,

$$k_{\mathrm{f}} = k_{\mathrm{E}}^{\mathrm{o}} \eta_{\mathrm{E}}^{-\alpha_{\mathrm{E,rds}}} \tag{25}$$

$$k_{\mathrm{b}} = k_{\mathrm{E}}^{\mathrm{o}} \eta_{\mathrm{E}}^{1-\alpha_{\mathrm{E,rds}}} \tag{26}$$

where $k^{\mathrm{o}}_{\mathrm{E}}$ is the standard rate constant in the rds of the interfacial electron transfer of the enzyme at the electrode, $\eta_{\mathrm{E}} = \exp\left\{ \frac{n'_{\mathrm{E}} F}{RT} (E - E_{\mathrm{E}}^{\mathrm{o}\prime}) \right\}$, n'_{E} is the number of electrons in the rds of the heterogeneous electron transfer of the enzyme (generally $n'_{\mathrm{E}} = 1$), $E^{\mathrm{o}\prime}_{\mathrm{E}}$ is the formal potential in the rds of the enzyme, and $\alpha_{\mathrm{E,rds}}$ is the transfer coefficient in the rds of the enzyme. When $E \gg E^{\mathrm{o}\prime}_{\mathrm{E}}$, $i_{\text{elec-enz}}$ is limited to $\pm n_{\mathrm{S}} F A k_{\mathrm{c,DET}} \Gamma_{\mathrm{E}}$.

In addition, $k^{\mathrm{o}}_{\mathrm{E}}$ decreases exponentially with an increase in the distance between the electrode surface and an electrode-active site of the enzyme (*d*) [50-52]. Thus, DET-type bioelectrocatalysis is often improved by using mesoporous electrode materials on which enzymes adsorb in increased probability of orientations favorable for DET-type reactions. Suitable modification of the electrode surface with chemical substances leads to electrostatic or specific attractive interaction between the electrode surface and the enzyme surface close to the electrode-active site [14,30].

2.3. Examples of MET/DET-type biosensors

The most popular enzymatic biosensors are those for self-monitoring of blood glucose (SMBG); blood glucose concentration being an important index in the treatment of diabetes. Various types of amperometric glucose biosensors have been reported [53-59]. SMBG sensors involve FAD-dependent glucose oxidase (GOD) [60,61], bacterial and fungal FAD-dependent glucose dehydrogenase (FAD-GDH) [62,63], PQQ-dependent soluble GDH (PQQ-sGDH) [64-66], and NAD-dependent GDH (NAD-GDH) [67]. Characteristics of the enzymes are summarized in a review [68].

Kakehi et al. reported a biofuel cell-type glucose biosensor using bacterial flavohemo-GDH complex containing a cytochrome subunit as well as an FAD subunit. The authors proposed that the enzyme proceeded DET-type bioelectrocatalysis at the cytochrome subunit, and the open-circuit potential was used as a measure of the glucose concentration in the range of 0.5 mM to 6 mM [69].

Fructose biosensors are also useful in food analyses and diagnoses of kidney function. The sensors can be utilized for determining the inulin clearance, a difference of the intake and discharge of inulin filtered in the kidney, inulin being hydrolyzed into fructose and glucose by inulinase [70]. A membrane-bound flavohemo-enzyme, D-fructose dehydrogenase (FDH), catalyzes two-electron oxidation of D-fructose, shows high activity of DET-type bioelectrocatalysis, and is often mounted on fructose biosensors [71]. Both DET- and MET-type fructose biosensors are summarized in a review [72].

Cellobiose dehydrogenase (CDH) is useful for lactose biosensing [73]. CDH comprises an FAD-containing larger catalytic dehydrogenase domain and a heme *b*-containing smaller cytochrome domain that directly communicates with electrodes [73]. As a mimic of CDH, in addition, the cytochrome domain was introduced into some other flavoenzymes by protein engineering methods, and the engineered enzymes realized DET-type bioelectrocatalysis. Ito et al. designed a cytochrome domain-linked fungal FAD-GDH and constructed a DET-type amperometric glucose biosensor [74].

3. Multi-enzymatic cascades

3.1. Diaphorase/NAD(P)⁺-dependent enzymes

NAD(P)⁺/NAD(P)H is a natural coenzyme that is involved in a large variety of redox enzymes. Usually, NAD(P)(H) shuttle back and forth from NAD(P)-dependent enzymes and to the solution to transfer the hydride ion, like a mediator. However, NAD(P) is an unfavorable mediator in MET-type reactions for NAD(P)-dependent enzymes, because the direct electrochemical reaction of NAD(P)(H) at electrodes requires high overpotentials, because NAD(P) is not an electron carrier but a hydride ion carrier; electron-transfer characteristics are essential for electrode reactions. Therefore, other

additional mediators, such as Meldola's blue (MB) that can undergo both hydride ion and electron transfers, were used as mediators. It shows large values of the second-order reaction rate constant with NAD(P)H (hydride ion transfer) and also the heterogeneous electron transfer rate constant with electrodes (electron transfer) [75]. Avramescu et al. constructed a D-lactate biosensor using NAD-dependent D-lactate dehydrogenase (D-LDH), NAD(H), and MB, with a detection limit of 0.05 mM, a linear range of 0.1–1 mM, and a sensitivity of 1.2 µA cm^{-2} mM^{-1} [76].

Furthermore, FMN-containing diaphorase (DI) that catalyzes a redox reaction between NAD(P)(H) and a mediator can be utilized to build up more efficient mediated systems and was introduced in MET-type biosensors using NAD-dependent enzymes [77-80]. Takagi et al. analyzed bi-enzymatic MET-type bioelectrocatalysis of NAD-dependent L-lactate dehydrogenase (L-LDH) and DI using several mediators (Fig. 2A) [77]. The bi-enzyme system realized an interconversion (bi-way conversion) between L-lactate and pyruvate. Nikitina et al. reported an amperometric formaldehyde biosensor with NAD-dependent formaldehyde dehydrogenase, DI, and an osmium redox polymer, with a detection limit of 32 µM, a linear range of 50–500 µM, and a sensitivity of 2.2 µA cm^{-2} mM^{-1} [79].

On the other hand, Siritanaratkul et al. reported a DET-type interconversion of NADP$^+$/NADPH catalyzed by ferredoxin-NADP$^+$ reductase (FNR) [81]. They also demonstrated L-glutamate synthesis from 2-oxoglutarate and NH$_4^+$ by the coupled reactions of FNR and NADP-dependent glutamate dehydrogenase (GLDH) [81]. Multi-enzymatic biosensors using FNR have not yet been reported, but a DET-type NADP$^+$/NADPH interconversion by FNR might be useful for constructing NADP-dependent enzymatic biosensors without any additional mediators (Fig. 2B).
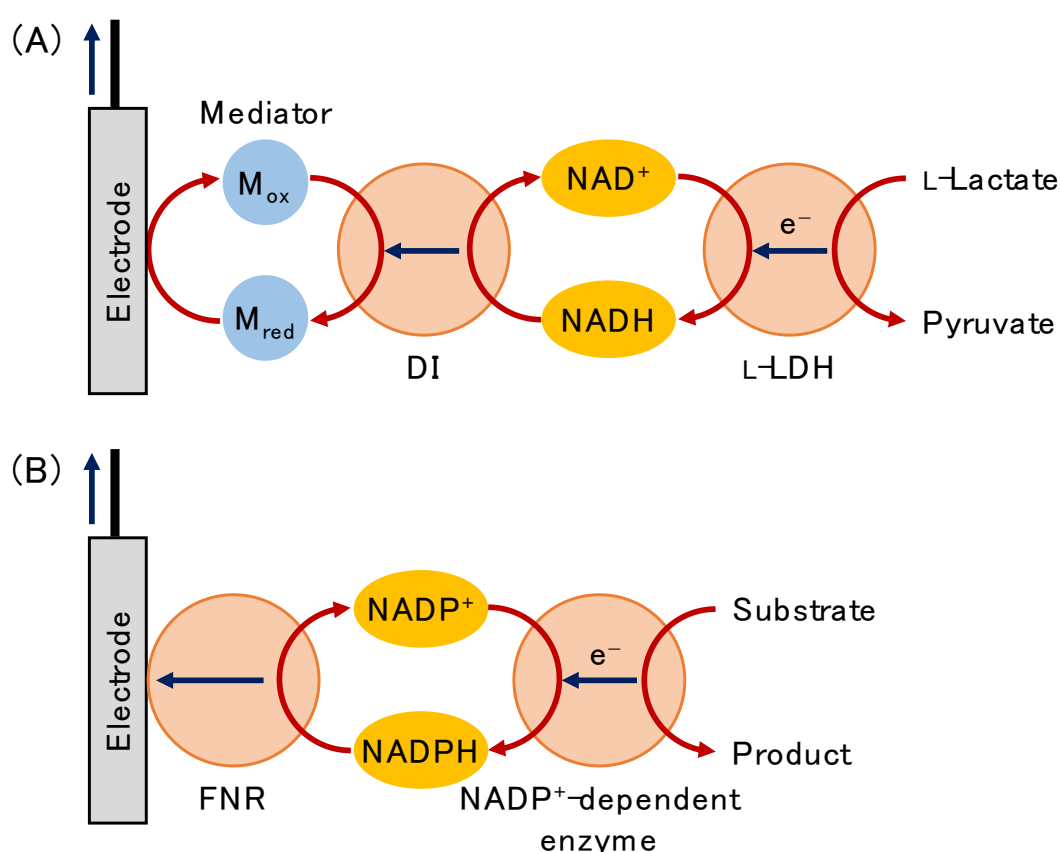

Figure. 2.   (A) A schematic view of MET-type bioelectrocatalysis of L-LDH and DI.   (B) A schematic view of bi-enzymatic bioelectrocatalysis using an NADP$^+$-dependent enzyme and FNR.

3.2. Peroxidase/Oxidases

Several oxidases (ODs) were used as bioelectrocatalysts of 1st generation biosensors, which can detect and quantify target compounds by direct electrochemical oxidation of the enzymatically

generated hydrogen peroxide (H_2O_2) to dioxygen (O_2) [82-84]. However, direct oxidation of H_2O_2 at the electrode surface requires high overpotentials, and thus these biosensors are sensitive to interference by coexisting reductants [83,84].

In order to overcome this issue, H_2O_2 generated in an OD reaction was reductively detected with a help of horseradish peroxidase (HRP) that catalyzes two-electron reduction of H_2O_2 to H_2O. The HRP reaction was frequently coupled with electrode reactions in a way of MET-type bioelectrocatalysis. The two-enzyme coupled electrode may be called OP-type biosensors, here. In OP-type biosensors, the following reactions proceed;

$$S \;+\; O_2 \;\xrightarrow{\text{OD}}\; P \;+\; H_2O_2, \tag{27}$$

$$H_2O_2 + 2H^+ + 2e^- \xrightarrow{\text{HRP/electrode}} 2H_2O, \tag{28}$$
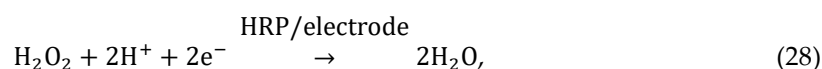
By introducing HRP, H_2O_2 detection at lower potentials was realized and the interference from other substances was reduced. The ODs mounted on OP-type biosensors reported so far are as follows: GOD [85,86], galactose oxidase (GalOD) [87], D- and L-amino acid oxidase [85,88,89], L-glutamate oxidase [90], amine oxidase [91], alcohol oxidase [85,91,92-95], urate oxidase [96], zinc superoxide dismutase [97], and so on. Castillo et al. also investigated the bioelectrocatalytic characteristics of sweet potato peroxidase (SPP), and SPP-based OP-type biosensors showed higher performance than HRP-based ones [91].

In addition, multi-enzymatic biosensors were constructed by incorporating upstream enzymatic reactions in OP-type biosensors. Tkáč et al. constructed a glucose non-interference lactose biosensor by introducing β-galactosidase, which hydrolyzes lactose to galactose and glucose, into the GalOD-HRP system [98]. Several groups reported cholesterol oxidase/cholesterol esterase/HRP co-immobilized biosensors, which enabled to monitor total cholesterol [99-101]. On the other hand, Nieh et al. reported a multi-enzymatic creatinine biosensor, as shown in Fig. 3 [102].

Recently, it was found that HRP showed a DET-type bioelectrocatalytic activity at mesoporous carbon and nanostructured gold electrodes [103,104], and 3rd generation OP-type biosensors using the DET-type reaction of HRP were reported. Xia et al. reported glucose and putrescine biosensors using GOD and putrescine oxidase, respectively [41,103]. In addition, Kawai et al. constructed an analytical model of an OP-type pyruvate biosensor based on the serial resistance concept [44].
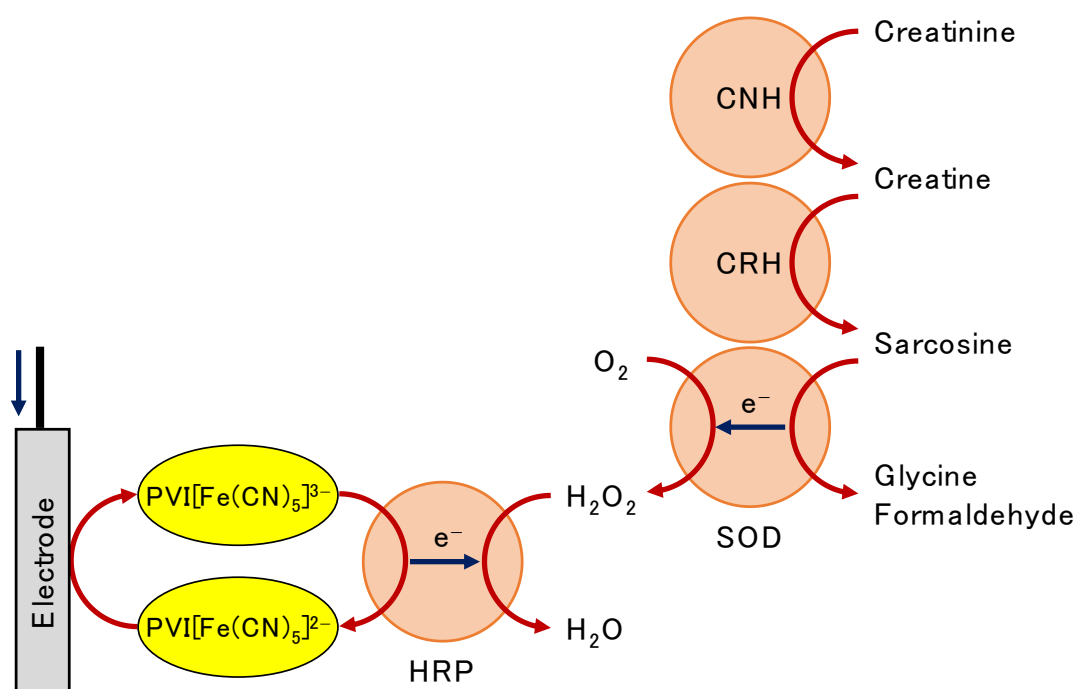
Figure. 3. A schematic view of multi-enzymatic creatinine biosensor. CNH, CRH, SOD and PVI[Fe(CN)$_5$]$^{2-/3-}$ indicate creatinine amidohydrolase, creatine amidohydrolase, sarcosine oxidase, and pentacyanoferrate-bound poly(1-vinylimidazole), respectively.

4. Multi-analyte detection

Real samples are mixtures containing multiple components. Especially, biological samples have complex compositions and relationship among the compositions remains unclear. In addition, there are many diseases of which the specific biomarker has not found out. Status of the human health is often evaluated on the basis of the balance of the compositions of the body fluid. Therefore, the multi-analyte sensing and monitoring of biological samples, that is, big data in human health attracted attention [105-107]. Similarly, multi-analyte detection in environmental samples is also an important subject [108]. Electrochemical sensors are easily miniaturized and compatible with such multi-analyte detection [109-111]. The development of printing technologies reduces the cost of the fabrication of bioelectrochemical sensors and realize a disposable sensor array system with a complicated structure. In this section, some notes in simultaneous multi-component measurements are outlined.

4.1. Crosstalk among amperometric biosensors

Electrical circuits of the amperometric sensors are on the basis of potentiostat. In the simplest construction of potentiostat, the working electrode set to common potential [112]. The circuit functions to maintain the potential difference between the working and reference electrodes at the setting potential by current flowing. Therefore, it is basically impossible to employ multiple working electrodes and a single pair of reference and counter electrodes by multiple potentiostats. Moreover, when the multiple electrochemical systems locate in a sample solution, the unnoticed electric connection of the potentiostats (for example, sharing ground) possibly causes the current flow between the working electrodes. In order to avoid these problems in the simultaneous measurements, it is necessary to employ a special apparatus (it is called multipotentiostat).

The desorption of enzymes and mediators from the electrode surface also becomes the origin of crosstalk among the sensing devices in sensors for multi-analyte detection. The immobilization of enzymes and mediators and employment of the permeable membrane are effective to reduce this type of crosstalk. In the disposable biosensor array, the design and layout of the sensors at the sensing device are important to prevent the cross-contamination within the measurement period.

4.2 Absolute and relative concentration

In order to reduce the damage of the subjects in sampling, discharged body fluids such as saliva, sweat, tear, and urine are better samples than blood. The homeostasis of the blood is important in the living things, while the water contents in such discharged body fluids change readily with time, movement, and uptake, et al. Therefore, the determination of the relative concentration of the components to the internal standard becomes more important than the determination of the absolute concentration of the components in the body fluids. Here, the homeostasis of the internal standard will become problems, because its concentration affects all over the measurements. Furthermore, the calibration of the individual sensors is a fatal problem, because the calibration process of the sensor for the multiple-analyte is incompatible with the disposable sensors. Calibration of the sensors is required if the sensitivities of sensors are unstable. Therefore, the stability of the sensor is important in disposable sensors.

4.3 Examples of the internal standard in body fluids

The most widely used internal standard in the urine sample is creatinine. Creatinine is a metabolite of creatine in muscle. The produced creatinine transfers from blood to urine through the kidney. The steady-state production of creatinine in the human body is widely accepted. Therefore, in the blood of healthy people, the concentration of creatinine is practically constant and the amount of transferred creatinine into urine is also constant. In urine analysis, creatinine is usually employed

for calibration of the other components. However, since renal dysfunction causes the variation of creatinine concentration in urine, creatinine is not a perfect standard [113].

The water content in sweat is easily varied. The suggested internal standards in sweat are chloride ion [114] and sodium ion [115]. Because it is difficult to incorporate those ions into the redox reaction, potentiometry is suitable to detect these ions.

In the metabolism of human bodies, L-lactate is a normal product. However, bacteria can produce both D- and L-lactates. Therefore, D-lactate in body fluids is a marker for bacterial infection [116]. In order to remove the dilution effect of body fluid, the most suitable reference material is L-lactate. Therefore, the simultaneous detection of lactate enantiomers is the most effective construction. In order to determine the D/L ratio of lactate in body fluid, the combination of the diffusion limited amperometric D- and L-lactate sensors was reported based on MET-type bioelectrocatalysis of corresponding NAD-dependent enzymes and MB [43].

5. Prospective biosensors without calibration

Biosensors are fundamentally fragile, due to enzyme properties. The functions of biomaterials are easily suppressed by acid, base, oxidation, heat, dehydration, and other external factors. Because the sensitivities of biosensors are generally subjected to change, frequent calibrations of biosensors may be required to guarantee accuracy. In this section, prospective biosensors without calibration are introduced.

5.1 Significance of mass-transfer controlling

As mentioned above, the current response of an amperometric biosensor is expressed as a serial combination of each reaction step. A simple case of the substrate reductive MET-type biosensing employing rotating disk electrode is considered here.

As mentioned in Section 2, the response of biosensors is affected by many physical quantities. However, the stability or reproducibility of these quantities is different from each other in the constructed biosensors. The features of the selectable or controllable values are summarized in Table 1. Generally, the electrode area (A) is easy to control except for nanoelectrodes. The formal potential of the mediator ($E_M^{o\prime}$) is possible to control by the selection of the mediator. Since the stability of redox mediators are limited due to oxygen and light damage, it is difficult to define the rigid redox state of mediators. Since the stability of the reference electrode is frequently poor, the value of E is unstable. The lack of uniformity of permeable membranes causes the poor reproducibility of P_m. The rotating speed is easy to control. The most unstable component in the biosensor is enzymes. The value of $k_c \Gamma_E$ decreases by the denaturation of the enzyme with time. Therefore, the mass transfer process is the most stable and controllable in amperometric biosensors. The stabilization of biosensors must be achieved by setting the mass transfer process as the rate-determining step.

Table 1. Physical quantities affected to the amperometric biosensing.

Physical quantities	Stability	Reproducibility	controllability
A	good	good	good
$E_M^{o\prime}$	good	good	poor
c_M	poor	good	good
E	poor	poor	good
P_m	good	poor	poor
ω	good	good	good
$k_c \Gamma_E$	poor	poor	poor

5.2 Bioelectrocatalysis at microelectrodes

As described in the above (Section 2), the steady-state mass transfer from the solution to an electrode is realized by rotating electrodes or microelectrodes. However, since the rotating electrode

requires a special apparatus, the application in the biosensors for real sample measurements seems to be difficult. Therefore, microelectrodes are more suitable for construction for amperometric biosensors. Another advantage of microelectrodes is a high signal-noise ratio because of the relatively high Faradaic current density against the charging current density.

Microelectrodes are classified into some types based on the symmetry of the shape, such as microsphere, microdisk, microcylinder, and microband [112]. The microdisk electrode is the most available microelectrode. The time-dependence of the limited current of a microdisk electrode (i_{md}) with a radius of r is given as follows [117],

$$i_{\mathrm{md}} = 4 n_{\mathrm{S}} F D_{\mathrm{S}} c_{\mathrm{S}} r \left\{ 0.7854 + 0.8862 \sqrt{\tau_{\mathrm{d}}} + 0.2146 \exp\left(-\frac{0.7823}{\sqrt{\tau_{\mathrm{d}}}} \right) \right\}, \qquad (29)$$

where τ_{d} is the dimensionless time for the microdisk and is defined as follows:

$$\tau_{\mathrm{d}} = \frac{4 D_{\mathrm{S}} t}{r^2}. \qquad (30)$$

At the long-time limitation ($t \to \infty$), the current reaches a steady-state value given by Eq. (15); the mass-transfer-limited current density at the microdisk electrode increases with a decrease in the radius of the electrode. On the other hand, the enzymatic reaction-limited current density would be constant at a constant surface density of the enzyme. Therefore, it would become difficult to satisfy the requirement for diffusion-controlled biosensors ($i_{\mathrm{enz}} \gg i_{\mathrm{mt,microdisk}}$) at microdisk electrodes with extremely small values of r. Similar situation is expected for micro-rode electrodes. In other words, most of the microelectrode-type biosensors are often controlled by the enzymatic kinetics (or the permeability of the outer membrane, if any), and therefore the response would be subjected to change. However, if one can realize extremely fast enzymatic reactions on microelectrodes, one may satisfy the condition: $i_{\mathrm{enz}} \gg i_{\mathrm{mt,microdisk}}$.

The simplest case is extremely fast DET-type bioelectrocatalysis at a microdisk electrode. In this situation, the substrate concentration at the microelectrode surface is regarded as zero, that is, diffusion-controlled limiting current conditions are realized. Some of multicopper-oxidases (MCOs) reduce oxygen to water at the surface of mesoporous electrodes by DET-type bioelectrocatalysis with sufficiently high activity. Mass-transfer-controlled DET-type bioelectrocatalysis was realized at MCO-modified porous gold microdisk electrodes [118]. The porous electrode was employed to increase the effective surface area and the probability of orientations suitable for DET-type bioelectrocatalysis thanks to curvature effects [19,119,120]. Figure 4A shows voltammograms recorded at a Cu-efflux oxidase-modified porous gold microelectrode (solid line) with and (dotted line) without oxygen. The sigmoidal curve indicates the DET-type bioelectrocatalysis of oxygen reduction. A clear potential-independent limiting current was observed. The limiting current linearly increased with the bulk concentration of oxygen, as shown in Fig. 4B. The solid line in Fig. 4B shows the theoretical sensitivity calculated with Eq. (15) using the literature value of D_{S} and the microscopically measured r. The agreement between the experimental and theoretical sensitivities verifies that the response of the constructed oxygen sensor is truly controlled by the mass transfer of oxygen. Since the sensitivity of the sensor is independent of the activity of CueO, the sensor has excellent reproducibility and stability at a constant temperature.
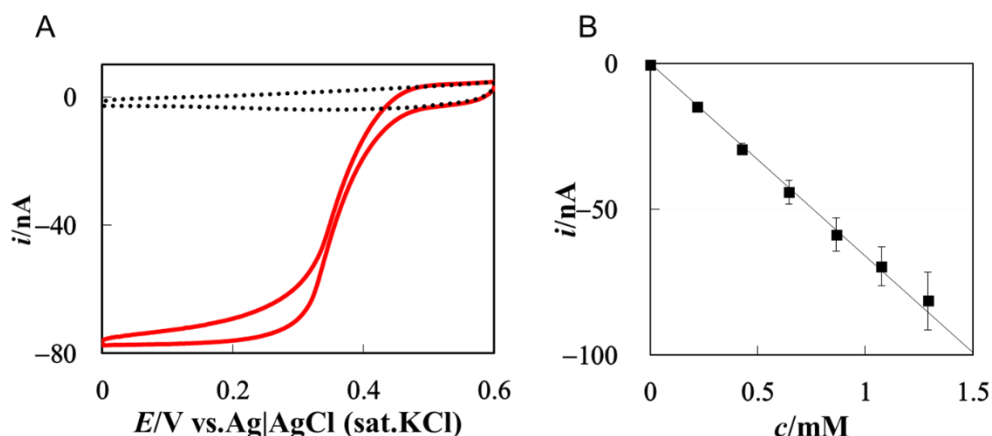
Figure 4. (A) Cyclic voltammogram of CueO modified porous gold microdisk electrode recorded with r = 20 μm (solid line) with and (dotted line) without oxygen. (B) (Squares) experimental and (solid line) theoretical calibration curve for the Oxygen biosensor. Reprinted from Ref. 118, Copyright (2020), with permission from Elsevier.

The situation of MET-type bioelectrocatalysis at a microelectrode is more complicated than that of DET-type bioelectrocatalysis due to the diffusion of the mediator. However, when a large amount of active enzymes exist in the system, it is possible to realize the substrate-diffusion-controlled MET-type bioelectrocatalysis at a microdisk electrode. According to this concept, a MET-type glucose sensor was constructed using a microdisk electrode, 1,2-benzoquinone, and FAD-GDH [39]. The current response quickly reached a steady-state (Fig. 5). The linear range of the sensor was from 0 mM to 3 mM of glucose while the concentration of the mediator is 1 mM in the system (inset in Fig. 5). Obviously, the linear range is beyond the endpoint situation. Moreover, the current response of the sensor agreed with the diffusion-controlled value of glucose.
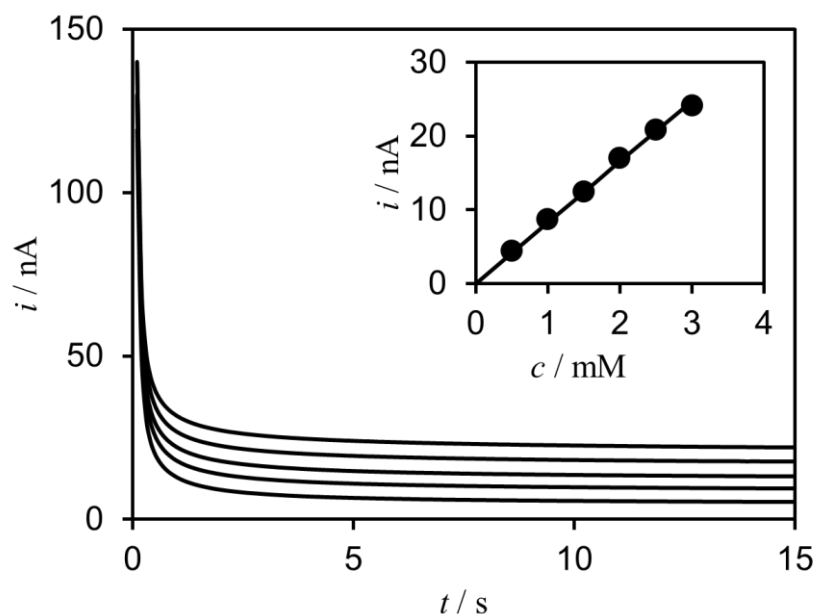

Figure 5. Chronoamperometric response for glucose oxidation in a buffer solution containing 0.21 mM FAD-GDH and 1 mM 1,2-benzoquinone at a microelectrode with diameter of 50μm. Inset shows the calibration curve based on the current at 10 s. Reprinted with permission from Ref. 39, Copyright (2013) Japan Society for Analytical Chemistry.

The situation where the MET-type bioelectrocatalysis occurs around a microelectrode was simulated by the finite element method [40]. The concentration profiles of the substrate, reduced form of the mediator, and reduced enzyme are given in Fig. 6 under the conditions that the enzymatic reaction is extremely fast. While the concentration gradient of the substrate spreads hemispherically, the concentration gradient of the mediator is located only in the vicinity of the electrode surface. The concentration profile of the enzyme clearly shows the enzymatic reaction occurs only in the thin region (as a reaction plane) where the enzyme concentration gradient exists. The flux of the substrate is quickly converted to that of the mediator in the thin region. Therefore, the surface of the thin region plays the role of a virtual electrode that selectively reacts with the substrate. The increase in the substrate concentration leads to a decrease in the distance of the thin region and then increases the current density.
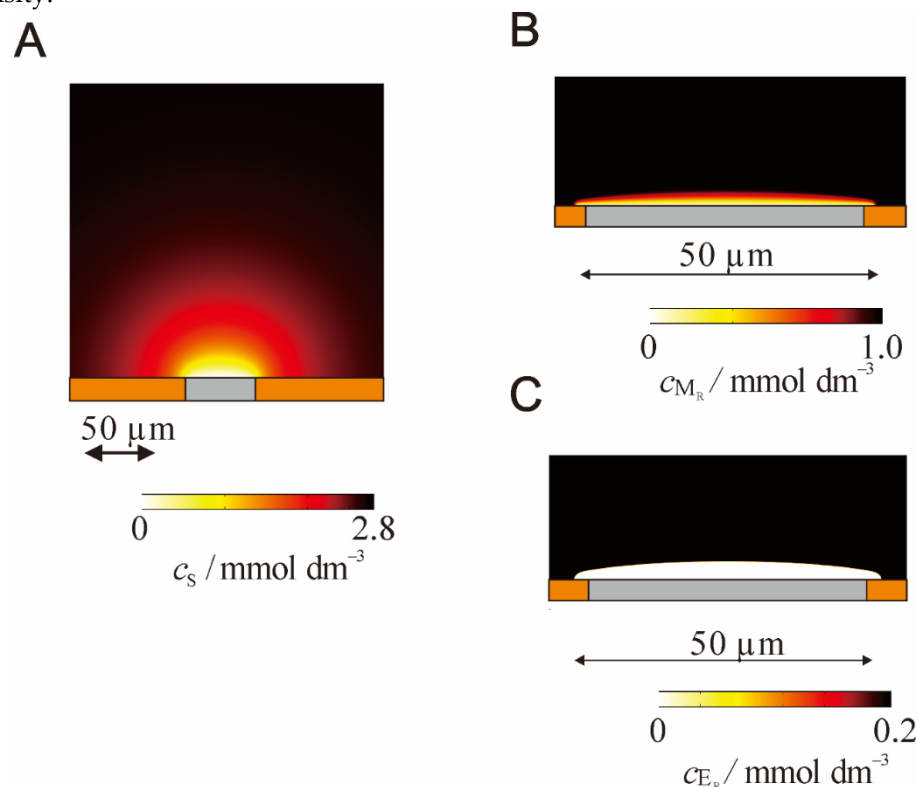
Figure 6. Concentration profiles of (A) substrate, (B) reduced mediator, and (C) reduced form of enzyme around an microdisk electrode with r = 25 μm at a substrate concentration of 4 mmol dm^{-3}, a mediator concentration of 1 mmol dm^{-3}, an enzyme concentration of 0.2 mmol dm^{-3}. The profiles were calculated for the situation of 20 s after the potential step at the limiting current conditions. Reprinted from Ref. 40 with permission from the PCCP Owner Societies.

5.3 Pseudo-steady-state response

Although microdisk electrodes provide clear steady-state current, the current is quite small. In order to increase the current, microdisk electrode array without overlapping of the diffusional concentration gradients (scattered microdisk electrode array) is one of the solutions [38,121-123]. However, the fabrication of such a scattered microdisk electrode array is a technically challenging issue. Another solution to increase the current may be the employment of microband electrodes. Ultrathin-ring electrodes can be considered as rod electrodes [124,125]. The time-dependence of the limiting current at a microband electrode (i_{mb}) with a length of l and a thickness of w is given by [126]:

$$i_{mb} = n_S F D_S c_S l \left[\frac{\pi \exp\left(-\frac{2}{5}\sqrt{\pi\tau_b}\right)}{4\sqrt{\pi\tau_b}} + \frac{\pi}{\ln\left\{64\tau_b \exp(-0.5772156) + \exp\left(\frac{5}{3}\right)\right\}} \right], \quad (31)$$

where τ_b is the non-dimensional time for the band electrode and is defined as follows,

$$\tau_b = \frac{D_S t}{w^2}. \tag{32}$$

According to Eq. (31), i_{mb} easily magnifies with an increase in *l*. On the other hand, i_{mb} becomes 0 at $t \rightarrow \infty$. Therefore, the exact analysis of i_{mb} based on the steady-state current is not possible. However, the decay of i_{mb} is so slow that the current is practically indistinguishable from the so-called steady-state current. In actual electrochemical measurements, a quasi-steady-state response is acceptable for practical use. For example, MET-type bioelectrocatalysis of FAD-GDH at microband electrodes provides the values very close to the diffusion-limited response [42].

Since the current density at a microelectrode is quite large, the mass-transfer limited bioelectrocatalysis is fundamentally difficult. Therefore, a relatively large microelectrode ($r = 1.5$ mm) is promising to realize the mass-transfer limited bioelectrocatalysis. In Eq. (29), time is a dimensionless quantity and the scale is determined by *r*. Therefore, Eq. (29) is more suitable to define the limiting current decay at a disk electrode than the Cottrell equation. The current decay given by Eq. (29) is slower than that of the Cottrell equation. Even if the electrode radius is few mm, the limiting current reaches quasi-steady-state values. The quasi-steady-state characteristics of a disk electrode ($r = 1.5$ mm) realized diffusion-controlled lactate biosensing [43].

5.4 Potentiometric coulometry

Coulometry is one of the absolute quantification methods and the most accurate electroanalytical methods in theory. In coulometry, the charge (electricity) due to the objective redox reaction is measured. Coulometry coupled with bioelectrocatalysis is a familiar technique [127-131]. However, small Faradaic current compared with the non-Faradaic current at porous electrodes causes a decrease in the accuracy of bioelectrocatalytic coulometry.

On the other hand, potentiometry is expected to avoid the effect of non-Faradaic current. When redox mediators exist in the solution, the redox enzymatic reaction with the mediator changes the ratio of the oxidized and reduced forms of the mediator. The change of the ratio changes the solution potential based on the Nernst equation. When the redox mediator is immobilized at the electrode surface in a thin layer, the change of the ratio of the oxidized and reduced forms of the mediator (Γ_O/Γ_R) changes the electrode potential (*E*). If the total amount of immobilized mediator ($A\Gamma_T$) is constant, the accumulated charge (Q_S) is evaluated directly from the initial value and equilibrated value of *E* (E_i and E_f, respectively) as follows;

$$Qs = \frac{-n_M F A \Gamma_T}{1 + \exp\left[\frac{n_M F}{RT}(E_f - E^{\circ\prime})\right]} + \frac{n_M F A \Gamma_T}{1 + \exp\left[\frac{n_M F}{RT}(E_i - E^{\circ\prime})\right]}. \tag{33}$$

However, in the case of osmium complex polymer as a mediator immobilized at the electrode surface, the relationship between *E* and Γ_O/Γ_R was deviated from the Nernst equation [45]. The strong electrostatic interactions between the redox sites in the polymer are the most possible cause. An increase in the ionic strength in the medium will decrease the electrostatic interaction between the redox species at the electrode surface. In order to increase the ionic strength, a redox active thin liquid film containing a highly concentrated electrolyte solution was fabricated on the electrode surface [46]. Figure 7 shows the construction of the liquid film-modified electrode. The components of the thin liquid film were a hydrophobic ionic liquid (1-ethyl-3-methylimidazolium bis(nonafluorobutanesulfonyl)imide), organic medium (dibutyl phthalate), and a redox mediator (ferrocene). Ferrocene is enzymatically oxidized at the surface of the liquid film by H_2O_2 with peroxidase (POD). Since the electrostatic interaction was effectively suppressed, the liquid film-modified electrode played as a reversible and ideal surface-confined system. Since the value of $A\Gamma_T$ is controlled in the fabrication of the modified electrode, the value of Q_S by the bioelectrocatalysis can be estimated from Eq. (33) without any calibration.

The sensitivity of the potentiometric coulometry could be regulated on the basis of the value of $A\Gamma_T$. Since no current flows across the system, the interference due to the non-Faradaic processes could be eliminated by potentiometric coulometry.
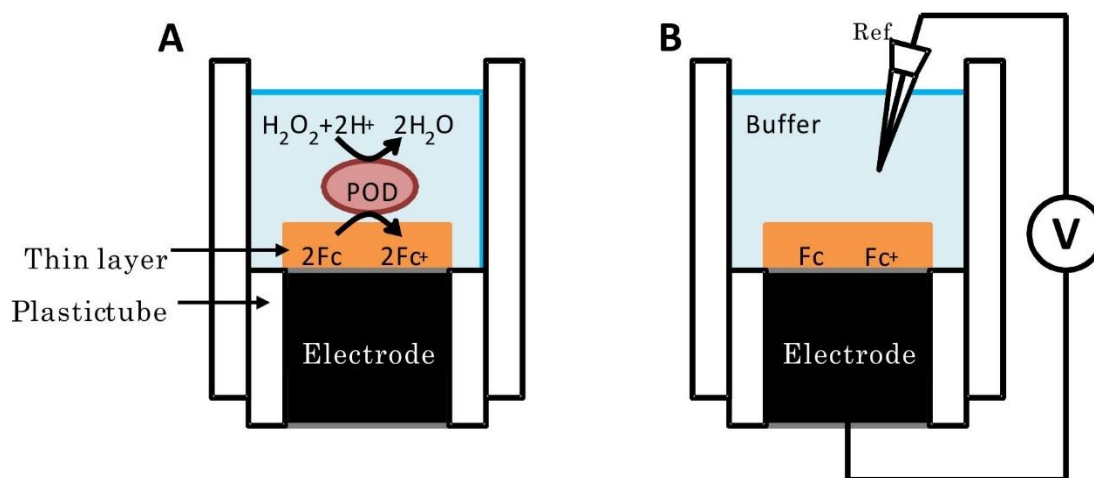

Figure 7. Schematic illustrations of (A) the accumulation process and (B) the potentiometric measurement of a liquid-film-modified electrode. Reprinted from Ref. 46, Copyright (2015), with permission from Elsevier.

6. Conclusions

Over the past few decades in the field of bioelectrochemistry, several attempts have been conducted to utilize redox enzymes as electrocatalysts and to develop novel bioelectrochemical systems. By comparison with inorganic catalysts, redox enzymes have distinctive characteristics such as high activity, extremely large size, identity by regeneration, uniformity, versatility, and fragility. In this review, we provide an overview and additional insights and discuss the recent progress on the practical use of amperometric biosensors such as multi-enzyme biosensors, multi-analyte biosensors. Prospective diffusion-controlled biosensors based on DET- and MET-type reactions and potentiometric coulometry based on MET-type reaction may be utilized without calibration. All these efforts may be useful for constructing bioelectrochemical sensors for practical use.

References

[1]   Bartlett, P.N. Bioelectrochemistry: Fundamentals, Experimental Techniques and Applications. John Wiley & Sons, Chichester 2008.

[2]   Wilson, G.S.; Johnson, M.A. In-vivo Electrochemistry: What Can We Learn about Living Systems? *Chem. Rev.* **2008**, *108*, 2462–2481.

[3]   Heller, A. Electrical Connection of Enzyme Redox Centers to Electrodes. *J. Phys. Chem.* **1992**, *96*, 3579–3587.

[4]   Thévenot, D.R.; Tóth, K.; Durst, R.A.; Wilson, G. Electrochemical Biosensors: Recommended Definitions and Classification. *Pure Appl. Chem.* **1999**, *71*, 2333–2348.

[5]   Armstrong, F.A.; J. Hinst, Reversibility and Efficiency in Electrocatalytic Energy Conversion and Lessons from Enzymes. *Proc. Natl. Acad. Sci. USA.* **2011**, *108*, 14049–14054.

[6]   de Poulpiquet, A.; Ranava, D.; Monsalve, K.; Giudici-Orticoni, M.-T.; Lojou, E. Biohydrogen for a New Generation of H_2/O_2 Biofuel Cells: A Sustainable Energy Perspective. *ChemElectroChem* **2014**, *1*, 1724–1750.

[7]   Fourmond, V.; Léger, C. Modelling the Voltammetry of Adsorbed Enzymes and Molecular Catalysts. *Curr. Opin. Electrochem.* **2017**, *1*, 110–120.

[8]   Martinkova, P.; Kostelnik, A.; Valek, T.; Pohanska, M. Main Streams in the Construction of Biosensors and Their Applications. *Int. J. Electrochem. Sci.* **2017**, *12*, 7386–7403.

[9]   Bollella, P.; Gorton, L. Enzyme Based Amperometric Biosensors, *Curr. Opin. Electrochim.* **2018**, *10*, 157–173.

[10] Kano, K. Fundamentals and Applications of Redox Enzyme-Functionalized Electrode Reactions. *Electrochemistry* **2019**, *87*, 301–311.

[11] Kucherenko, I.S.; Soldatkin, O.O.; Kucherenko, D.Y.; Soldatkina, O.V.; Dzyadevych, S.V. Advances in Nanomaterial Application in Enzyme-Based Electrochemical Biosensors. *Nanoscale Adv.* **2019**, *1*, 4560–4577.

[12] Ngyen, H.H.; Lee, S.H.; Lee, U.J.; Fermin, C.D.; Kim, M. Immobilized Enzymes in Biosensor Applications. *Materials* **2019**, *12*, 121.

[13] Pinyou, P.; Blay, V.; Muresan, L.M.; Noguer, T. Enzyme-Modified Electrodes for Biosensors and Biofuel Cells. *Mater. Horiz.* **2019**, *6*, 1336–1358.

[14] Bollella, P.; Katz, E. Enzyme-Based Biosensors: Tackling Electron Transfer Issues. *Sensors* **2020**, *20*, 3517.

[15] Willner, I.; Katz, E.; Willner, B. Electrical Contact of Redox Enzyme Layers Associated with Electrodes; Routes to Amperometric Biosensors, *Electroanalysis* **1997**, *9*, 965–977.

[16] Barton, S.C.; Gallaway, J.; Atanassov, P. Enzymatic Biofuel Cells for Implantable and Microscale Devices. *Chem. Rev.* **2004**, *104*, 4867–4886.

[17] Cracknell, J.A.; Vincent, K.A.; Armstrong, F.A. Enzymes as Working or Inspirational Electrocatalysts for Fuel Cells and Electrolysis. *Chem. Rev.* **2008**, *108*, 2439–2461.

[18] Meredith, M. T.; Minteer, S. D. Biofuel Cells; Enhanced Enzymatic Bioelectrocatalysis, *Annu, Rev. Anal. Chem.* **2012**, *5*, 157–179.

[19] Mazurenko, I.; de Poulpiquet, A.; Lojou, E. Recent Developments in High Surface Area Bioelectrodes for Enzymatic Fuel Cells. *Curr. Opin. Electrochem.* **2017**, *5*, 74–84.

[20] Mano, N.; de Poulpiquet, A. O_2 Reduction in Enzymatic Biofuel Cells. *Chem. Rev.* **2018**, *118*, 2392–2468.

[21] Krieg, T.; Sydow, A.; Schröder, U.; Schrader, J.; Holtmann, D. Reactor Concepts for Bioelectrochemical Syntheses and Energy Conversion. *Trends Biotechnol.* **2014**, *32*, 645–655.

[22] Milton, R.D.; Minteer, S.D. Enzymatic Bioelectrosynthetic Ammonia Production: Recent Electrochemistry of Nitrogenase, Nitrate Reductase, and Nitrite Reductase. *ChemPlusChem* **2017**, *82*, 513–521.

[23] Shleev, S.; González-Arribas, E.; Falk, M. Biosupercapacitors. *Curr. Opin. Electrochem.* **2017**, *5*, 226–233.

[24] Dutton, P.L. Redox Potentiometry: Determination of Midpoint Potentials of Oxidation-Reduction Components of Biological Electron-Transfer Systems. *Methods in Enzymology* 1**978**, *54*, 411–435.

[25] Scheller, F.; Kirstein, D.; Kirstein, L.; Schubert, F.; Wollenberger, U.; Olsson, B.; Gorton, L.; Johansson, G. Enzyme Electrodes and Their Application. *Phil. Trans. R. Lond. B.* **1987**, *316*, 85–94.

[26] Scheller, F.; Schubert, F.; Pfeiffer, D.; Hintsche, R.; Dransfeld, I.; Renneberg, R.; Wollenberger, U.; Riedel, K.; Pavlova, M.; Kühn, M.; Müller, H.-G.; Tan, P.M.; Hoffmann, W.; Moritz, W. Research and Development of Biosensors. *Analyst* **1989**, *114*, 653–662.

[27] Freìre, R.S.; Pessoa, C.A.; Mello, L.D.; Kubota, L.T. Direct Electron Transfer: An Approach for Electrochemical Biosensors with Higher Selectivity and Sensitivity. *J. Braz. Chem. Soc.* **2003**, *14*, 230–243.

[28] Léger, C.; Bertrand, P. Direct Electrochemistry of Redox Enzymes as Tool for Mechanistic Studies. *Chem. Rev.* **2008**, *108*, 2379–2438.

[29] Milton, R.D.; Minteer, S.D. Direct Enzymatic Bioelectrocatalysis: Differentiating between Myth and Reality. *J. R. Soc. Interface* **2017**, *14*, 20170253.

[30] Adachi, T.; Kitazumi, Y.; Shirai, O.; Kano, K. Direct Electron Transfer-Type Bioelectrocatalysis of Redox Enzymes at Nanostructured Electrodes. *Catalysts* **2020**, *10*, 236.

[31] Kitazumi, Y.; Shirai, O.; Kano, K. Significance of Nanostructures of an Electrode Surface in Direct Electron Transfer-Type Bioelectrocatalysis of Redox Enzymes, in Novel Catalyst Materials for Bioelectrochemical Systems: Fundamentals and Applications. ACS publications, Washington, DC, 2020.

[32] Hooda, V.; Gahlaut, A.; Gothwal, A.; Hooda, V. Recent Trends and Perspectives in Enzyme Based Biosensor Development for the Screening of Triglycerides: A Comprehensive Review. *Artif. Cells Nanomed. Biotechnol.* **2018**, *46*, 626–635.

[33] Semenova, D.; Gernaey, K.V.; Morgan, B.; Silina, Y.E. Towards One-Step Design of Tailored Enzymatic Nanobiosensors. *Analyst* **2020**, *145*, 1014–1024.

[34] Pilas, J.; Yazici, Y.; Selmer, T.; Keusgen, M.; Schöning, M.J. Application of a Portable Multi-Analyte Biosensor for Organic Acid Determination in Silage. *Sensors* **2018**, *18*, 1470.

[35] Zhu, L.; Yang, R.; Zhai, J.; Tian, C. Bienzymatic Glucose Biosensor Based on Co-Immobilization of Peroxidase and Glucose Oxidase on a Carbon Nanotubes Electrode. *Biosens. Bioelectron.* **2007**, *23*, 528–535.

[36] Jia, F.; Narasimhan, B.; Mallapragada, S. Materials-Based Strategies for Multi-Enzyme Immobilization and Co-Localization. *Biotechnol. Bioeng.* **2013**, *111*, 209–222

[37] Serafin, V.; Hernández, P.; Agüí, L.; Yáñez-Sedeño, P.; Pingarrón, J.M. Electrochemical Biosensor for Creatinine Based on the Immobilization of Creatininase, Creatinase and Sarcosine Oxidase onto a Ferrocene/Horseradish Peroxidase/Gold Nanoparticles/Multi-Walled Carbon Nanotubes/Teflon Composite Electrode. *Electrochim. Acta* **2013**, *97*, 175–183.

[38] Noda, T.; Hamamoto, K.; Tsutumi, M.; Tsujimura, S.; Shirai, O.; Kano, K. Bioelectrocatalytic Endpoint Assays Based on Steady-State Diffusion Current at Microelectrode Array. *Electrochem. Commun.* **2010**, *12*, 839–842.

[39] Noda, T.; Wanibuchi, M.; Kitazumi, Y.; Tsujimura, S.; Shirai, O.; Yamamoto, M.; Kano, K. Diffusion-Controlled Detection of Glucose with Microelectrodes in Mediated Bioelectrocatalytic Oxidation. *Anal. Sci.*, **2013**, *29*, 279–281.

[40] Kitazumi, Y.; Noda, T.; Shirai, O.; Yamamoto, M.; Kano, K. Characteristics of Fast Mediated Bioelectrocatalytic Reaction near Microelectrodes. *Phys. Chem. Chem. Phys.* **2014**, *16*, 8905–8910.

[41] Xia, H.-Q.; Kitazumi, Y.; Shirai, O.; Ohta, H.; Kurihara, S.; Kano, K. Putrescine Oxidase/Peroxidase-Co-Immobilized and Mediator-Less Mesoporous Microelectrode for Diffusion-Controlled Steady-State Amperometric Detection of Putrescine. *J. Electroanal. Chem.* **2017**, *804*, 128–132.

[42] Matsui, Y.; Hamamoto, K.; Kitazumi, Y.; Shirai, O.; Kano, K. Diffusion-Controlled Mediated Electron Transfer-Type Bioelectrocatalysis Using Ultrathin-Ring and Microband Electrodes as Ultimate Amperometric Glucose Sensors. *Anal. Sci.*, **2017**, *33*, 845–851.

[43] Matsui, Y.; Kitazumi, Y.; Shirai, O.; Kano, K. Simultaneous Detection of Lactate Enantiomers Based on the Diffusion-Controlled Bioelectrocatalysis. *Anal. Sci.* **2018**, *34*, 1137–1142.

[44] Kawai, H.; Kitazumi, Y.; Shirai, O.; Kano, K. Performance Analysis of an Oxidase/Peroxidase-Based Mediatorless Amperometric Biosensor. *J. Electroanal. Chem.* **2019**, *841*, 73–78.

[45] Nieh, C.-H.; Kitazumi, Y.; Shirai, O.; Yamamoto, M.; Kano, K. Potentiometric Coulometry Based on Charge Accumulation with a Peroxidase/Osmium Polymer-Immobilized Electrode for Sensitive Determination of Hydrogen Peroxide. *Electrochem. Commun.* **2013**, *33*, 135–137.

[46] Katsube, R.; Kitazumi, Y.; Shirai, O.; Yamamoto, M.; Kano, K. Potentiometric Coulometry Using a Liquid-Film-Modified Electrode as a Reversible Surface-Confined System. *J. Electroanal. Chem.* **2016**, *780*, 114–118.

[47] Matsumoto, R.; Kano, K.; Ikeda, T. Theory of Steady-State Catalytic Current of Mediated Bioelectrocatalysis. *J. Electroanal. Chem*. **2002**, 535, 37–40.

[48] Albery, W.J.; Cass, A.E.G.; Shu, Z.X. Inhibited Enzyme Electrodes. Part 1: Theoretical Model. *Biosens. Bioelectron.* **1990**, *5*, 367–378.

[49] Tsujimura, S.; Nakagawa, T.; Kano, K.; Ikeda, T. Kinetic Study of Direct Bioelectrocatalysis of Dioxygen Reduction with Bilirubin Oxidase at Carbon Electrodes. *Electrochemistry* **2004**, *72*, 437–439.

[50] Moser, C.C.; Keske, J.M.; Warncke, K.; Farid, R.S.; Dutton, P.L. Nature of Biological Electron Transfer. *Nature* **1992**, *355*, 796–802.

[51] Marcus, R.A.; Sutin, N. Electron Transfers in Chemistry and Biology. *BBA Rev. Bioenerg.* **1985**, *811*, 265–322.

[52] Marcus, R.A.; Electron Transfer Reactions in Chemistry: Theory and Experiment. *Angew. Chem. Int. Ed.* **1993**, *32*, 1111–1121.

[53] Wang, J. Electrochemical Glucose Biosensors. *Chem. Rev.* **2008**, *108*, 814–825.

[54] Heller, A.; Feldman, B. Electrochemical Glucose Sensors and Their Applications in Diabetes Management. *Chem. Rev.* **2008**, *108*, 2482–2505.

[55] Chen, C.; Xie, Q.; Yang, D.; Xiao, H.; Fu, Y.; Tan, Y.; Yao, S. Recent Advances in Electrochemical Glucose Biosensors. *RSC Advances* **2013**, *3*, 4473–4491.

[56] Zhu, Z.; Garcia-Gancedo, L.; Flewitt, A.J.; Xie, H.; Moussy, F.; Milne, W.I. A Critical Review of Glucose Biosensors Based on Carbon Nanomaterials: Carbon Nanotubes and Graphene. *Sensors* **2012**, *12*, 5996–6022.

[57] Lai, J.; Yi, Y.; Zhu, P.; Shen, J.; Wu, K.; Zhang, L.; Liu, J. Polyaniline-Based Glucose Biosensor. *J. Electroanal. Chem.* **2016**, *782*, 138–153.

[58] Rahman, M.M.; Ahammad, A.J.S.; Jin, J.-H.; Ahn, S.J.; Lee, J.-J. A Comprehensive Review of Glucose Biosensors Based on Nanostructured Metal-Oxides. *Sensors* **2010**, *10*, 4855–4886.

[59] Rahman, G.; Mian, S.A. Recent Trends in the Development of Electrochemical Glucose Biosensors. *Int. J. Biosen. Bioelectron.* **2017**, *3*, 210–213.

[60] Gregg, B.A.; Heller, A. Cross-Linked Redox Gels Containing Glucose Oxidase for Amperometric Biosensor Applications. *Anal. Chem.* **1990**, *62*, 258–263.

[61] Trifonov, A.; Stemmer, A.; Tel-Vered, R. Enzymatic Self-Wiring in Nanopores and Its Application in Direct Electron Transfer Biofuel Cells. *Nanoscale Adv.* **2019**, *1*, 347–356.

[62] Yamashita, Y.; Ferri, S.; Huynh, M.L.; Shimizu, H.; Yamaoka, H.; Sode, K. Direct Electron Transfer Type Disposable Sensor Strip for Glucose Sensing Employing an Engineered FAD Glucose Dehydrogenase. *Enzyme Microb. Technol.* **2013**, *52*, 123–128.

[63] Tsujimura, S.; Kojima, S.; Kano, K.; Ikeda, T.; Sato, M.; Sanada, H.; Omura, H. Novel FAD-Dependent Glucose Dehydrogenase for a Dioxygen-Insensitive Glucose Biosensor. *Biosci. Biotechnol. Biochem.* **2006**, *70*, 654–659.

[64] Malinauskas, A.; Kuzmarskyte, J.; Meskys, R.; Ramanavicius, A. Bioelectrochemical Sensor Based on PQQ-Dependent Glucose Dehydrogenase. *Sens. Actuators B* **2004**, *100*, 387–394.

[65] Flexer, V.; Durand, F.; Tsujimura, S.; Mano, N. Efficient Direct Electron Transfer of PQQ-Glucose Dehydrogenase on Carbon Cryogel Electrodes at Neutral pH. *Anal. Chem.* **2011**, *83*, 5721–5727.

[66] Bollella, P.; Lee, I.; Blaauw, D.; Katz E. A Microelectronic Sensor Device Powered by a Small Implantable Biofuel Cell. *ChemPhysChem* **2020**, *21*, 120–128.

[67] Mie, Y.; Yasutake, Y.; Ikegami, M.; Tamura, T. Anodized Gold Surface Enables Mediator-Free and Low-Overpotential Electrochemical Oxidation of NADH: A Facile Method for the Development of an NAD+-Dependent Enzyme Biosensor. *Sens. Actuators B* **2019**, *288*, 512–518.

[68] Ferri, S.; Kojima, K.; Sode, K. Review of Glucose Oxidases and Glucose Dehydrogenases: A Bird's Eye View of Glucose Sensing Enzymes. *J. Diabetes Sci. Technol.* **2011**, *5*, 1068–1076.

[69] Kakehi, N.; Yamazaki, T.; Tsugawa, W.; Sode, K. A Novel Wireless Glucose Sensor Employing Direct Electron Transfer Principle Based Enzyme Fuel Cell. *Biosens. Bioelectron.* **2007**, *22*, 2250–2255.

[70] Roe, J.H.; Epstein, J.H.; Goldstein, N.P. A Photometric Method for the Determination of Inulin in Plasma and Urine. *J. Biol. Chem.* **1949**, *178*, 839–845.

[71] Bollella, P.; Hibino Y.; Kano, K.; Gorton L.; Antiochia R. Highly Sensitive Membraneless Fructose Biosensor Based on Fructose Dehydrogenase Immobilized onto Aryl Thiol Modified Highly Porous Gold Electrode: Characterization and Application in Food Samples. *Anal. Chem.* **2018**, *90*, 12131–12136.

[72] Adachi, T.; Kitazumi, Y.; Shirai, O.; Kano, K. Bioelectrocatalytic Performance of D-Fructose Dehydrogenase. *Bioelectrochemistry* **2019**, *129*, 1–9.

[73] Bollella, P.; Ludwig, R.; Gorton, L. Cellobiose Dehydrogenase: Insights on the Nanostructuration of Electrodes for Improved Development of Biosensors and Biofuel Cells. *Appl. Mater. Today* **2017**, *9*, 319–332.

[74] Ito, K.; Okuda-Shimazaki, J.; Mori, K.; Kojima, K.; Tsugawa, W. Ikebukuro, K.; Lin, C.-E.; La Belle, J.; Yoshida, H.; Sode, K. Designer Fungus FAD Glucose Dehydrogenase Capable of Direct Electron Transfer. *Biosens. Bioelectron.* **2019**, *123*, 114–123.

[75] Gorton, L.; Torstensson, A.; Jaegfeldt, H.; Johansson, G. Electrocatalytic Oxidation of Reduced Nicotinamide Coenzymes by Graphite Electrodes Modified with an Adsorbed Phenoxazinium Salt, Meldola Blue. *J. Electroanal. Chem.* **1984**, *161*, 103–120.

[76] Avramescu, A.; Noguer, T.; Magearu, V.; Marty, J.-L. Chronoamperometric Determination of D-Lactate Using Screen-Printed Enzyme Electrodes. *Anal. Chim. Acta* **2001**, *433*, 81–88.

[77] Takagi, K.; Kano, K.; Ikeda, T. Mediated Bioelectrocatalysis Based on NAD-Related Enzymes with Reversible Characteristics. *J. Electroanal. Chem.* **1998**, *445*, 211–219.

[78] Antiochia, R.; Gallina, A.; Lavagnini, I.; Magno, F. Kinetic and Thermodynamic Aspects of NAD-Related Enzyme-Linked Mediated Bioelectrocatalysis. *Electroanalysis* **2002**, *14*, 1256–1261.

[79] Nikitina, O.; Shleev, S.; Gayda, G.; Demkiv, O.; Gonchar. M.; Gorton, L.; Csöregi, E.; Nistor, M. Bi-Enzyme Biosensor Based on NAD$^+$- and Glutathione-Dependent Recombinant Formaldehyde Dehydrogenase and Diaphorase for Formaldehyde Assay. *Sens. Actuators B* **2007**, *125*, 1–9.

[80] Lobo, M.J.; Miranda, A.J.; Tuñón, P. Amperometric Biosensors Based on NAD(P)-Dependent Dehydrogenase Enzymes. *Electroanalysis* **1997**, *9*, 191–201.

[81] Siritanaratkul, B.; Megarity, C.F.; Roberts, T.G.; Samuels, T.O.M.; Winkler, M.; Warner, J.H.; Happe, T.; Armstrong, F.A. Transfer of Photosynthetic NADP$^+$/NADPH Recycling Activity to a Porous Metal Oxide for Highly Specific, Electrochemically-Driven Organic Synthesis. *Chem. Sci.* **2017**, *8*, 4579–4586.

[82] Xu, C.X.; Marzouk, S.A.M.; Cosofret, V.V.; Buck, R.P.; Neuman, M.R.; Sprinkle, R.H. Development of a Diamine Biosensor. Talanta **1997**, *44*, 1625–1632.

[83] Carsol, M.-A.; Mascini, M.; Diamine Oxidase and Putrescine Oxidase Immobilized Reactors in Flow Injection Analysis: A Comparison in Substrate Specificity. *Talanta* **1999**, *50*, 141–148.

[84] Nagy, L.; Nagy, G.; Gyurcsanyi, R.E.; Neuman, M.R.; Lindner, E. Development and Study of an Amperometric Biosensor for the in Vitro Measurement of Low Concentration of Putrescine in Blood. *J. Biochem. Biophys. Methods* **2002**, *53*, 165–175.

[85] Gorton, L.; Jönsson-Pettersson, G.; Csöregi, E.; Johansson, K.; Domínguez, E.; Marko-Varga, G. Amperometric Biosensors Based on an Apparent Direct Electron Transfer between Electrodes and Immobilized Peroxidases. Plenary Lecture. *Analyst* **1992**, *117*, 1235–1241.

[86] Matsumoto, R.; Mochizuki, M.; Kano, K.; Ikeda, T. Unusual Response in Mediated Biosensors with an Oxidase/Peroxidase Bienzyme System. *Anal. Chem.* **2002**, *74*, 3297–3303.

[87] Tkáč, J.; Gemeiner, P.; Šturdík, E. Rapid and Sensitive Galactose Oxidase-Peroxidase Biosensor for Galactose Detection with Prolonged Stability. *Biotechnol. Tech.* **1999**, *13*, 931–936.

[88] Nieh, C.-H.; Kitazumi, Y.; Shirai, O.; Kano K. Sensitive D-Amino Acid Biosensor Based on Oxidase/Peroxidase System Mediated by Pentacyanoferrate-Bound Polymer. *Biosens. Bioelectron.* **2013**, *47*, 350–355.

[89] Kacaniklic, V.; Johansson, K.; Marko-Varga, G.; Gorton, L.; Jönsson-Pettersson, G.; Csöregi, E. Amperometric Biosensors for Detection of L- and D-Amino Acids Based on Coimmobilized Peroxidase and L- and D-Amino Acid Oxidases in Carbon Paste Electrodes. *Electroanalysis* **1994**, *6*, 381–390.

[90] Yoshida, S.; Kanno, H.; Watanabe, T. Glutamate Sensors Carrying Glutamate Oxidase/Peroxidase Bienzyme System on Tin Oxide Electrode. *Anal. Sci.* **1995**, *11*, 251–256.

[91] Castillo, J.; Gáspár, S.; Sakharov, I.; Csöregi, E. Bienzyme Biosensors for Glucose, Ethanol and Putrescine Built on Oxidase and Sweet Potato Peroxidase. *Biosens. Bioelectron.* **2003**, *18*, 705–714.

[92] Vijayakumar, A.R.; Csöregi, E.; Heller, A.; Gorton, L. Alcohol Biosensors Based on Coupled Oxidase-Peroxidase Systems. *Anal. Chim. Acta* **1996**, *327*, 223–234.

[93] Hasunuma, T.; Kuwabata, S.; Fukusaki, E.; Kobayashi, A. Real-Time Quantification of Methanol in Plants Using a Hybrid Alcohol Oxidase−Peroxidase Biosensor. *Anal. Chem.* **2004**, *76*, 1500–1506.

[94] Johansson, K.; Jönsson-Pettersson, G.; Gorton, L.; Marko-Varga, G.; Csöregi, E. A Reagentless Amperometric Biosensor for Alcohol Detection in Column Liquid Chromatography Based on Co-Immobilized Peroxidase and Alcohol Oxidase in Carbon Paste. *J. Biotechnol.* **1993**, *31*, 301–316.

[95] Smutok, O.; Ngounou, B.; Pavlishko, H.; Gayda, G.; Gonchar, M.; Schuhmann, W. A Reagentless Bienzyme Amperometric Biosensor Based on Alcohol Oxidase/Peroxidase and an Os-Complex Modified Electrodeposition Paint. *Sens. Actuators B* **2006**, *113*, 590–598.

[96] Akyilmaz, E.; Sezgintürk, M.K.; Dinçkaya, E. A Biosensor Based on Urate Oxidase−Peroxidase Coupled Enzyme System for Uric Acid Determination in Urine. *Talanta* **2003**, *61*, 73–79.

[97] Dharmapandian, P.; Rajesh, S.; Rajasingh, S.; Rajendran, A.; Karunakaran, C. Electrochemical Cysteine Biosensor Based on the Selective Oxidase–Peroxidase Activities of Copper, Zinc Superoxide Dismutase. *Sens. Actuators B* **2010**, *148*, 17–22.

[98] Tkáč, J.; Šturdík, E.; Gemeiner, P. Novel Glucose Non-Interference Biosensor for Lactose Detection Based on Galactose Oxidase–Peroxidase with and without Co-Immobilised β-Galactosidase. *Analyst* **2000**, *125*, 1285–1289.

[99] Crumbliss, A.L.; Stonehuerner, J.G.; Henkens, R.W.; Zhao, J.; O'Daly, J.P. A Carrageenan Hydrogel Stabilized Colloidal Gold Multi-Enzyme Biosensor Electrode Utilizing Immobilized Horseradish Peroxidase and Cholesterol Oxidase/Cholesterol Esterase to Detect Cholesterol in Serum and Whole Blood. *Biosens. Bioelectron.* **1993**, *8*, 331–337.

[100] Li, G.; Liao, J.M.; Hu, G.Q.; Ma, N.Z.; Wu, P.J. Study of Carbon Nanotube Modified Biosensor for Monitoring Total Cholesterol in Blood. *Biosens. Bioelectron.* **2005**, *20*, 2140–2144.

[101] Singh, S.; Solanki, P.R.; Pandey, M.K.; Malhotra, B.D. Cholesterol Biosensor Based on Cholesterol Esterase, Cholesterol Oxidase and Peroxidase Immobilized onto Conducting Polyaniline Films. *Sens. Actuators B* **2006**, *115*, 534–541.

[102] Nieh, C.-H.; Kitazumi, Y.; Shirai, O.; Kano K. Amperometric Biosensor Based on Reductive H_2O_2 Detection Using Pentacyanoferrate-Bound Polymer for Creatinine Determination. *Anal. Chim. Acta* **2013**, *767*, 128–133.

[103] Xia, H.-Q.; Kitazumi, Y.; Shirai, O.; Kano, K. Direct Electron Transfer-Type Bioelectrocatalysis of Peroxidase at Mesoporous Carbon Electrodes and Its Application for Glucose Determination Based on Bienzyme System. *Anal. Sci.* **2017**, *33*, 839–844.

[104] Sakai, K.; Kitazumi, Y.; Shirai, O.; Kano K. Nanostructured Porous Electrodes by the Anodization of Gold for an Application as Scaffolds in Direct-Electron-Transfer-Type Bioelectrocatalysis. *Anal. Sci.* **2018**, *34*, 1317–1322.

[105] Sadik, O.A.; Aluoch, A.O.; Zhou, A. Status of Biomolecular Recognition Using Electrochemical Techniques. *Biosens. Bioelectron.* **2009**, *24*, 2749–2765.

[106] Andreu-Perez, J; Poon, C.C.Y.; Merrifield, R.D.; Wong, S.T.C.; Yang G.-Z. Big Data for Health. *IEEE J. Biomed. Health* **2015**, *19*, 1193–1208.

[107] Tu, J.; Torrente-Rodríguez, R.M.; Wang, M.; Gao, W. The Era of Digital Health; A Review of Portable and Wearable Affinity Biosensors. *Adv. Funct. Mater.* **2020**, *30*, 1906713.

[108] March, G.; Nguyen, T.D.; Piro, B. Modified Electrodes Used for Electrochemical Detection of Metal Ions in Environmental Analysis. *Biosensors* **2015**, *5*, 241–275.

[109] Wang, J.; Katz, E. Digital Biosensors with Built-In Logic for Biomedical Applications–Biosensors Based on a Biocomputing Concept. *Anal. Bioanal. Chem.* **2010**, *398*, 1591–1603.

[110] Guz, N.; Halámek, J.; Rusling, J.F.; Katz, E. A Biocatalytic Cascade with Several Output Signals–Towards Biosensors with Different Levels of Confidence. *Anal. Bioanal. Chem.* **2014**, *406*, 3365–3370.

[111] Katz, E.; Poghossian A.; Schöning M.J. Enzyme-Based Logic Gates and Circuits–Analytical Applications and Interfacing with Electronics. *Anal. Bioanal. Chem*. **2017**, *409*, 81–94.

[112]   Bard, A.J.; Faulkner, L.R. Electrochemical Methods: Fundamentals and Applications. Wiley, New York, 2001, 2nd ed.

[113]   Waikar, S.S.; Sabbisetti, V.S.; Bonventre, J.V. Normalization of Urinary Biomarkers to Creatinine during Changes in Glomerular Filtration Rate. *Kidney Int.* **2010**, *78*, 486–494.

[114]   Ganguly, A.; Rice, P.; Lin, K.-C.; Muthukumar, S., Prasad, S. A Combinatorial Electrochemical Biosensor for Sweat Biomarker Benchmarking. *SLAS Technol.* **2020**, *25*, 25–32.

[115]   Appenzeller, B.M.R.; Schummer, C.; Rodrigues, S.B.; Wennig, R. Determination of the Volume of Sweat Accumulated in a Sweat-Patch Using Sodium and Potassium as Internal Reference. *J. Chromatogr. B* **2007**, *852*, 333–337.

[116]   Smith, S.M.; Eng, R.H.K.; Buccini, F. Use of D-Lactic Acid Measurements in the Diagnosis of Bacterial Infections. *J. Infect. Dis.* **1986**, *154*, 658–664.

[117]   Shoup, D.; Szabo, A. Chronoamperometric Current at Finite Disk Electrodes. *J. Electroanal. Chem.* **1982**, *140*, 237–245.

[118]   Miyata, M.; Kitazumi, Y.; Shirai, O.; Kataoka, K.; Kano, K. Diffusion-Limited Biosensing of Dissolved Oxygen by Direct Electron Transfer-Type Bioelectrocatalysis of Multi-Copper Oxidases Immobilized on Porous Gold Microelectrodes. *J. Electroanal. Chem.* **2020**, *860*, 113895.

[119]   Sugimoto, Y.; Takeuchi, R.; Kitazumi, Y.; Shirai, O.; Kano, K. Significance of Mesoporous Electrodes for Noncatalytic Faradaic Process of Randomly Oriented Redox Proteins. *J. Phys. Chem. C* **2016**, *120*, 26270–26277.

[120]   Sugimoto, Y.; Kitazumi, Y.; Shirai, O.; Kano, K. Effects of Mesoporous Structures on Direct Electron Transfer-Type Bioelectrocatalysis: Facts and Simulation on a Three-Dimensional Model of Random Orientation of Enzymes. *Electrochemistry* **2017**, *85*, 82–87.

[121]   Lee, H.J.; Beriet, C.; Ferrigno, R.; Girault, H.H. Cyclic Voltammetry at a Regular Microdisc Electrode Array. *J. Electroanal. Chem.* **2001**, *502*, 138–145.

[122]   Ordeig, O.; del Campo, J.; Muñoz, F.X.; Banks, C.E.; Compton, R.G. Electroanalysis Utilizing Amperometric Microdisk Electrode Arrays. *Electroanalysis* **2007**, *19*, 1973–1986.

[123]   Guo, J.; Lindner, E. Cyclic Voltammograms at Coplanar and Shallow Recessed Microdisk ElectrodeAarrays: Guidelines for Design and Experiment. *Anal. Chem.* **2009**, *81*, 130–138.

[124]   Bixler, J.W.; Fifield, M.; Poler, J.C.; Bond, A.M.; Thormann, W. An Evaluation of Ultrathin Ring and Band Microelectrodes as Amperometric Sensors in Electrochemical Flow Cells. *Electroanalysis* **1989**, *1*, 23–33.

[125]   Kitazumi, Y.; Hamamoto, K.; Noda, T.; Shirai, O.; Kano, K. Fabrication and Characterization of Ultrathin-Ring Electrodes for Pseudo-Steady-State Amperometric Detection. *Anal. Sci.* **2015**, *31*, 603–607 (2015).

[126]   Szabo, A.; Cope, D.K.; Tallman, D.E.; Kovach, P.M.; Wightman, R.M. Chronoamperometric Current at Hemicylinder and Band Microelectrodes: Theory and Experiment. *J. Electroanal. Chem.* **1987**, *217*, 417–423.

[127]   Uchiyama, S.; Kato, S.; Suzuki, S.; Hamamoto, O. Biocoulometry of Cholesterol Using Porous Carbon Felt Electrodes. *Electroanalysis* **1991**, *3*, 59–62.

[128]   Morris, N.A.; Cardosi, M.F.; Birch, B.J.; Turner, A.P.F. An Electrochemical Capillary Fill Device for the Analysis of Glucose Incorporating Glucose Oxidase and Ruthenium (III) Hexamine as Mediator. *Electroanalysis* **1992**, *4*, 1–9.

[129]   Fukaya, M.; Ebisuya, H.; Furukawa, K.; Akita, S.; Kawamura, Y.; Uchiyama, S. Self-Driven Coulometry of Ethanol, D-Glucose and D-Fructose Using Ubiquinone-Dependent Dehydrogenase Reactions. *Anal. Chim. Acta* **1995**, *306*, 231–236.

[130]   Tsujimura, S.; Nishina, A.; Kamitaka, Y.; Kano, K. Coulometric D-Fructose Biosensor Based on Direct Electron Transfer Using D-Fructose Dehydrogenase. *Anal. Chem.* **2009**, *81*, 9383–9387.

[131]   Mizutani, F.; Kato, D.; Kurita, R.; Mie, Y.; Sato, Y.; Niwa, O. Highly-Sensitive Biosensors with Chemically-Amplified Responses. *Electrochemistry* **2008**, *76*, 515–521.